Combination of Factor H Mutation and Properdin Deficiency Causes Severe C3 Glomerulonephritis

Allison M. Lesher,* Lin Zhou,* Yuko Kimura,* Sayaka Sato,* Damodar Gullipalli,* Andrew P. Herbert,† Paul N. Barlow,† Hannes U. Eberhardt,‡ Christina Skerka,‡ Peter F. Zipfel,‡§ Takayuki Hamano,‖ Takashi Miwa,* Kenneth S. Tung,¶ and Wen-Chao Song*

*Department of Pharmacology and Institute for Translational Medicine and Therapeutics and ‖Center for Clinical Epidemiology and Biostatistics, Perelman School of Medicine, University of Pennsylvania, Philadelphia, Pennsylvania; †Edinburgh Biomolecular Nuclear Magnetic Resonance Unit, Centre for Chemical and Translational Biology, Schools of Biological Sciences and Chemistry, University of Edinburgh, Edinburgh, United Kingdom; ‡Department of Infection Biology, Leibniz Institute for Natural Product Research and Infection Biology, Hans Knöll Institute, Jena, Germany; §Friedrich Schiller University, Jena, Germany; and ¶Department of Pathology, University of Virginia School of Medicine, Charlottesville, Virginia

ABSTRACT

Factor H (fH) and properdin both modulate complement; however, fH inhibits activation, and properdin promotes activation of the alternative pathway of complement. Mutations in fH associate with several human kidney diseases, but whether inhibiting properdin would be beneficial in these diseases is unknown. Here, we found that either genetic or pharmacological blockade of properdin, which we expected to be therapeutic, converted the mild C3 GN of an fH-mutant mouse to a lethal C3 GN with features of human dense deposit disease. We attributed this phenotypic change to a differential effect of properdin on the dynamics of alternative pathway complement activation in the fluid phase and the cell surface in the fH-mutant mice. Thus, in fH mutation-related C3 glomerulopathy, additional factors that impact the activation of the alternative pathway of complement critically determine the nature and severity of kidney pathology. These results show that therapeutic manipulation of the complement system requires rigorous disease-specific target validation.

J Am Soc Nephrol 24: 53–65, 2013. doi: 10.1681/ASN.2012060570

Complement is a component of the innate immune system that plays a key role in recognizing and fighting pathogenic infections.[1,2] Three main pathways exist to initiate complement activation: the classic pathway, the lectin pathway, and the alternative pathway (AP). The classic and lectin pathways are initiated by antigen–antibody complexes and microbial sugar molecules, respectively. The AP is constitutively active at a low level caused by spontaneous C3 tick-over and capable of self-amplification on foreign surfaces that lack regulatory control.[1,2] Although complement plays a physiologic role in host defense and homeostasis, inappropriately activated complement can lead to serious tissue injury. In particular, AP dysregulation has been implicated in many complement-mediated human autoimmune disorders.[3–6]

AP complement activation is regulated by several membrane-bound and fluid-phase proteins. Among them, factor H (fH) is an abundant plasma regulator that works to restrict the activity of the C3 convertase C3bBb both on the cell surface and in the fluid phase.[7–9] It is a glycoprotein composed of 20 short consensus repeat (SCR) domains, and it inhibits the AP C3 convertase C3bBb by decay acceleration and

Received June 12, 2012. Accepted October 11, 2012.

Published online ahead of print. Publication date available at www.jasn.org.

Correspondence: Dr. Wen-Chao Song, University of Pennsylvania, Perelman School of Medicine, Room 1254 BRBII/III, 421 Curie Boulevard, Philadelphia, PA 19104. Email: songwe@upenn.edu

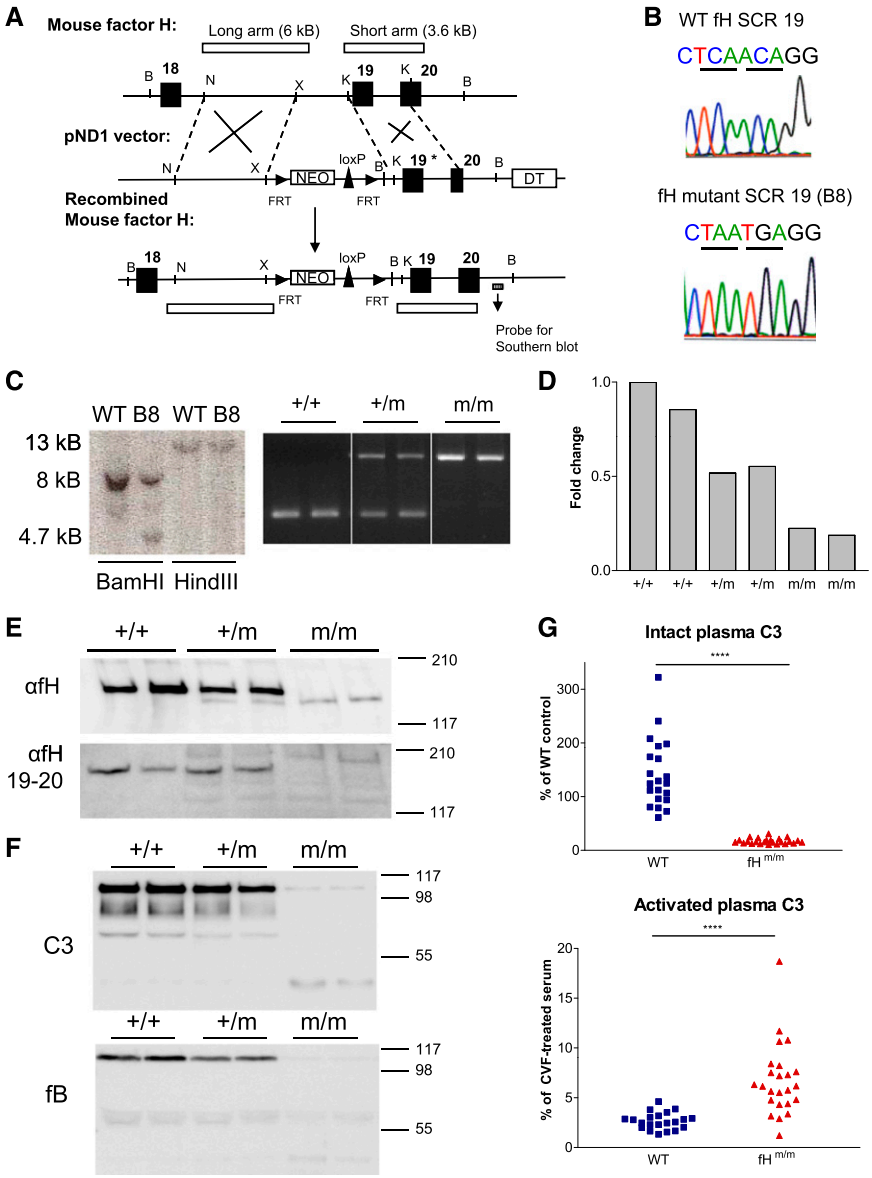

Figure 1. Generation of the fH mutant mouse (fH$^{m/m}$). (A) Gene targeting strategy for the mouse fH locus. Open boxes designate long and short arms for recombination. *Site of fH mutations. Other symbols include exons (■), loxP site (▲), and FRT sites (►). Restriction enzyme sites are abbreviated: B, *Bam*HI; K, *Kpn*I; N, *Not*I; X, *Xho*I. Other abbreviations include neomycin (NEO) and diphtheria toxin (DT). (B) Sequencing chromatograms of WT fH gene and the mutant fH allele from a positive ES cell clone confirming mutations in the fH SCR19 sequence. (C) Genotyping of WT and mutant ES cell clones and mice. (Left panel) Southern blot of ES cell genomic DNA digested with *Bam*HI showing the presence of a 4.7-kB band from the mutant allele of the fH gene. As expected, the targeted allele produced the same restriction digestion pattern as the WT allele when DNA was digested with *Hind*III. (Right panel) PCR genotyping using tail DNA of WT (+/+), heterozygous (+/m), and homozygous (m/m) fH mutant mice. (D) Real-time PCR analysis of relative fH mRNA levels in the liver of fH$^{m/m}$ mice and littermate controls. Each bar represents one mouse. Glyceraldehyde-3-phosphate dehydrogenase was used as an internal control, and all values were normalized to the values of WT mice. (E and F) Western blotting for (E) plasma fH and (F) C3 and fB in fH$^{m/m}$ mice and littermates. E shows Western blots using antibodies against either (upper panel) full-length or (lower panel) fH SCR19–20 of mouse fH. A small amount of truncated mouse fH was detected by anti-fH antibody but not the anti-fH SCR19–20 antibody in heterozygous and homozygous mutant mice. (G) Quantification of intact and activated plasma C3 by ELISA in WT (n=21) and fH$^{m/m}$ (n=24) mice. An arbitrary WT mouse plasma sample was used as a reference against which all intact C3 values were normalized. A CVF-treated mouse serum sample was used as a reference against which all activated C3 values were normalized. ****$P<0.0001$, t test.

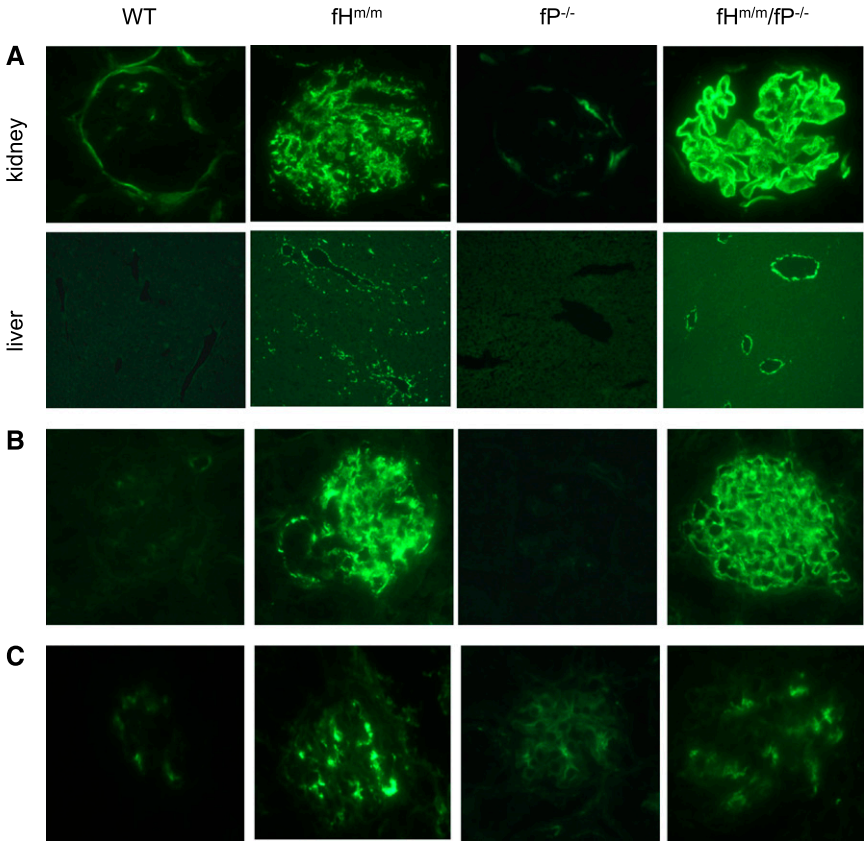

Figure 2. Immunofluorescent staining of C3, C9, and IgG in mouse kidney and liver sections. (A) Immunofluorescent staining of C3 in the kidney (×400) and liver (×200) sections of WT, fP$^{-/-}$, fH$^{m/m}$, and fH$^{m/m}$/fP$^{-/-}$ mice. (B) Immunofluorescent staining of C9 in the kidney sections (×400) of WT, fP$^{-/-}$, fH$^{m/m}$, and fH$^{m/m}$/fP$^{-/-}$ mice. (C) Immunofluorescent staining of IgG in the kidney sections (×400) of WT, fP$^{-/-}$, fH$^{m/m}$, and fH$^{m/m}$/fP$^{-/-}$ mice. Mice used were 2 months old.

cofactor activity for factor I (fI)-mediated proteolytic cleavage of C3b. The C-terminal SCR domains of fH interact with surface-deposited C3b and polyanionic molecules on eukaryotic cells, and they play a critical role in determining its affinity for host tissues.[10,11] The N-terminal 1–4 SCRs of fH are responsible for its complement-regulating activity. Opposing the activities of fH and other membrane complement regulators, factor properdin (fP) is a plasma protein that facilitates AP complement activation. It stabilizes the labile AP C3 convertase C3bBb, significantly extending its half-life.[12] Recent studies have shown that fP may also work as an initiator of AP complement on certain activating surfaces.[13–18] In contrast to the multitude of negative regulators, fP is the only known positive regulator of the complement cascade.

Mutations in fH in animals and man are associated with several kidney pathologies, including C3 GN, dense deposit disease (DDD), and atypical hemolytic uremic syndrome (aHUS).[9,19–21] Development of these diseases has also been linked to other abnormalities in AP complement regulation, such as the presence of nephritic factors and mutations in C3, factor B (fB), membrane cofactor protein, and fI.[22–24] Many of these disease-causing defects, including fH mutations, lack complete penetrance, and presently it is not well understood how disease phenotypes associated with these defects might be affected by other modifier genes or abnormalities. Here, we provide a striking example in mice, where loss of fP activity, while expected to be therapeutic, surprisingly converted a mild C3 GN phenotype of an fH mutant mouse to lethal C3 GN resembling human DDD. Our results shed new light on the pathogenesis of fH-related kidney diseases and have therapeutic implications for human C3 glomerulopathy patients.

RESULTS

Mice with an fH C-Terminal Mutation Develop C3 GN

fH mutations and deficiency are associated with several human kidney pathologies, including aHUS and C3 glomerulopathy.[23,25] In aHUS patients, mutations in fH are most frequently observed in SCR19–20, a region that has been shown by recent experiments to be critical for C3b and cell surface binding.[26,27] To generate a murine model of human aHUS, we used a gene-targeting approach to delete SCR19–20 of mouse fH. We introduced two stop codons to the beginning of SCR19 of the mouse fH gene (Figure 1, A and B) and obtained correctly targeted embryonic stem (ES) cells, from which homozygous fH mutant mice (fH$^{m/m}$) were produced (Figure 1C). Although we intended to use this strategy to generate a mouse with a truncated fH lacking SCR19–20, analysis of fH$^{m/m}$ mice unexpectedly revealed low levels of fH mRNA in the liver (Figure 1D). Correspondingly, only a small amount of the truncated fH protein was detected in the plasma of fH$^{m/m}$ mice (Figure 1E). As expected, the truncated fH was recognized by an antibody against full-length mouse fH but not an antibody raised against mouse fH SCR19–20 protein (Figure 1E). These observations led us to conclude that the nonsense mutations introduced to SCR19 drastically reduced fH expression, most likely as a result of mRNA instability.[28–30]

By ELISA and Western blot analysis, we detected only trace levels of intact C3 and fB but elevated levels of activated C3 in the plasma of fH$^{m/m}$ mice (Figure 1, F and G). These results suggested that the small amount of truncated fH was not sufficient to control spontaneous AP complement activation in fH$^{m/m}$ mice, and consequently, there was exhaustive consumption of AP complement components. This phenotype of fH$^{m/m}$ mice was reminiscent of the phenotype observed

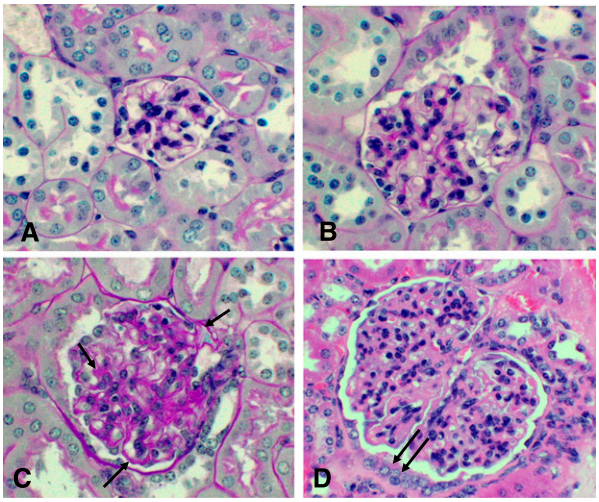

Figure 3. Kidney histology of $fH^{m/m}$ mice. On PAS staining, (A) 2-month-old WT mouse glomeruli had normal cellularity, whereas (B) age-matched $fH^{m/m}$ mouse glomeruli showed mild mesangial proliferation but had patent capillary loops. Pathologic features of C3 GN were evident on (C) PAS and (D) hematoxylin/eosin staining in 10- to 12-month-old $fH^{m/m}$ mice, including hypercellularity, GBM thickening (single arrows), and signs of early crescent formation (double arrows). Original magnification, ×400.

in fH knockout mice ($fH^{-/-}$) described previously.[31] Like $fH^{-/-}$ mice, $fH^{m/m}$ mice had prominent glomerular C3 and C9 deposition but weak IgG deposition (Figure 2). The identity of the glomerular IgG remains to be determined but is unlikely to be related to an autoimmune response to the mutant fH protein because we detected no serum autoantibodies against fH SCR1–18 (Supplemental Figure 1). At 2–3 months, $fH^{m/m}$ mice displayed mild glomerular hypercellularity and some evidence of inflammatory infiltrate (Figure 3B and Table 1), but glomerular histology under light microscopy was otherwise unremarkable at this age. By 10–12 months, most $fH^{m/m}$ mice had developed signs of GN, characterized by increased glomerular hypercellularity, inflammatory infiltrate, and thickening of glomerular basement membrane (GBM) (Figure 3, C and D and Table 1). In some mutant mice, early crescents consisting largely of tubular or parietal epithelial cells were also observed at this age (Figure 3C and Table 1). Heavy proteinuria was observed in 2 of 14 surviving $fH^{m/m}$ mice of this age, and it correlated with more severe renal pathology in these two animals (Table 1). Thus, although we intended to create an aHUS model, the $fH^{m/m}$ mouse that we engineered displayed an age-dependent C3 GN phenotype instead.

Deficiency of Properdin in $fH^{m/m}$ Mice Exacerbates C3 GN and Causes Early Death

Given that fP promotes AP complement activation and recent findings showed that fP targeting ameliorated tissue injury in several murine models of AP complement-mediated disease,[14,32–34] we speculated that C3 GN in $fH^{m/m}$ mice might be alleviated or prevented by fP deficiency. To test this hypothesis, we crossed the $fH^{m/m}$ mouse with an fP knockout mouse ($fP^{-/-}$) and generated $fH^{m/m}/fP^{-/-}$ mice. Contrary to our expectation, we found that $fH^{m/m}/fP^{-/-}$ mice all developed exacerbated C3 GN and died prematurely. Figure 4A shows an aggregate survival curve of multiple $fH^{m/m}/fP^{-/-}$ mouse cohorts compared with the survival curves of wild type (WT) and $fH^{m/m}$ controls. Although there was variation in the age of mortality, most $fH^{m/m}/fP^{-/-}$ mice died between 8 and 12 weeks, with none surviving beyond 5 months (Figure 4A). Analysis of a littermate cohort of WT, $fH^{m/m}$, and $fH^{m/m}/fP^{-/-}$ mice revealed that $fH^{m/m}/fP^{-/-}$ mice developed significant proteinuria at 6–8 weeks, whereas age-matched $fH^{m/m}$ mice showed no signs of protein leakage (Figure 4B). Consistent with the proteinuria data, we detected evidence of podocyte injury in $fH^{m/m}/fP^{-/-}$ mice by immunofluorescent staining of nephrin, a protein critical to the integrity of the glomerular filtration barrier. Nephrin is normally expressed at the slit diaphragm of podocyte foot processes. Loss of nephrin expression has been associated with podocyte injury and proteinuria in several studies.[35–37] We detected normal nephrin staining in the glomeruli of 8-week-old WT, $fP^{-/-}$, and $fH^{m/m}$ mice, but nephrin staining was significantly reduced in the glomeruli of age-matched $fH^{m/m}/fP^{-/-}$ mice (Supplemental Figure 2). In addition to displaying proteinuria, $fH^{m/m}/fP^{-/-}$ mice were hypercholesterolemic (Figure 4C), suggesting that they suffered from a nephrotic syndrome. Plasma albumin levels were also noticeably lower in $fH^{m/m}/fP^{-/-}$ mice (median=26.7 mg/ml, range=10.1–50.0 mg/ml; n=13) compared with age-matched WT (median=31.8 mg/ml, range=25.6–47.4 mg/ml; n=9) and $fH^{m/m}$ mice (median=34.7 mg/ml, range=21.8–46.7 mg/ml; n=16), although the difference did not reach statistical significance. Serum creatinine levels were not elevated in $fH^{m/m}/fP^{-/-}$ mice that appeared to be grossly normal but were markedly increased in moribund $fH^{m/m}/fP^{-/-}$ mice (Figure 4D), suggesting that $fH^{m/m}/fP^{-/-}$ mice died from renal failure.

Periodic acid-Schiff (PAS) staining of the kidney confirmed an exacerbated C3 GN phenotype in $fH^{m/m}/fP^{-/-}$ mice. At 8 weeks of age, WT and $fP^{-/-}$ glomeruli had normal cellularity and GBM structure with patent capillary loops (Figure 5, A and B). Some $fH^{m/m}$ glomeruli showed mild mesangial expansion but retained normal capillary loops and appeared largely healthy by light microscopy (Figure 3B). In contrast, 8-week-old $fH^{m/m}/fP^{-/-}$ mouse kidneys had significant thickening of the glomerular capillary walls, lobulation of glomeruli, mesangial proliferation, and glomerular leukocyte infiltration (Figure 5C). Parietal cell proliferation with protein globules was also observed in some $fH^{m/m}/fP^{-/-}$ mice by this age, and early glomerular crescent formation was seen as well (Figure 5D). C3 GN of similar severity was observed in $fH^{m/m}$ mice only when they had reached 10–12 months of age (Table 1). As in $fH^{m/m}$ mice, there was prominent C3 and C9 but minimal IgG deposition in the glomeruli of $fH^{m/m}/fP^{-/-}$ mice (Figure 2). $fH^{m/m}/fP^{-/-}$ mice eventually developed a fatal and rapidly

Table 1. Summary of kidney pathology in WT, $fP^{-/-}$, $fH^{m/m}$, and $fH^{m/m}/fP^{-/-}$ mice

Genotype	*n*	Mesangial Proliferation	Glomerular Inflammation	Endocapillary Proliferation	Glomerular Capillary Wall Thickening	Crescents	Glomeruli with Crescents (%)	Glomerular Sclerosis	Interstitial Inflammation	Area of Interstitial Fibrosis (%)	Arteriosclerosis
2–3 mo											
WT	7	0.0±0.0 (0/7)	0.0±0.0 (0/7)	0.0±0.0 (0/7)	0.0±0.0 (0/7)	0.0±0.0 (0/7)	0.0±0.0 (0/7)	0.0±0.0 (0/7)	0.0±0.0 (0/7)	0.0±0.0 (0/7)	0.0±0.0 (0/7)
$fP^{-/-}$	7	0.0±0.0 (0/7)	0.0±0.0 (0/7)	0.0±0.0 (0/7)	0.0±0.0 (0/7)	0.0±0.0 (0/7)	0.0±0.0 (0/7)	0.0±0.0 (0/7)	0.0±0.0 (0/7)	0.0±0.0 (0/7)	0.0±0.0 (0/7)
$fH^{m/m}$	9	1.4±0.1[a] (9/9)	0.0±0.0 (0/9)	0.0±0.0 (0/9)	0.0±0.0 (0/9)	0.0±0.0 (0/9)	0.0±0.0 (0/9)	0.0±0.0 (0/9)	0.0±0.0 (0/9)	0.0±0.0 (0/9)	0.0±0.0 (0/9)
$fH^{m/m}/fP^{-/-}$	5	2.1±0.3[b] (5/5)	0.6±0.6 (1/5)	0.4±0.4 (1/5)	0.6±0.4 (2/5)	0.4±0.4 (1/5)	3.2±3.2 (1/5)	0.0±0.0 (0/5)	0.0±0.0 (0/5)	2.0±2.0 (1/5)	0.0±0.0 (0/5)
$fH^{m/m}/fP^{-/-}$ (moribund)	5	1.6±0.2[a] (5/5)	2.8±0.2[c] (5/5)	3.0±0.0[c] (5/5)	2.4±0.2[c] (5/5)	3.5±0.3[c] (5/5)	80.6±6.7[c] (5/5)	2.2±0.3[c] (5/5)	3.8±0.2[c] (5/5)	65.0±7.4[c] (5/5)	0.4±0.4 (1/5)
10–12 mo											
WT	18	0.7±0.2 (10/18)	0.1±0.1 (1/18)	0.0±0.0 (0/18)	0.0±0.0 (0/18)	0.0±0.0 (0/18)	0.0±0.0 (0/18)	0.0±0.0 (0/18)	0.5±0.1 (12/18)	0.0±0.0 (0/18)	0.0±0.0 (0/18)
$fH^{m/m}$	14	2.4±0.2[d] (14/14)	2.0±0.2[d] (13/14)	2.4±0.3[d] (12/14)	1.8±0.2[d] (13/14)	0.4±0.3 (2/14)	9.1±6.6 (2/14)	0.3±0.2 (2/14)	0.8±0.2 (10/14)	2.9±1.9 (3/14)	0.0±0.0 (0/14)

Data are presented as mean ± SEM and number of mice affected (in parentheses) and analyzed among age-matched cohorts. One-way ANOVA with Tukey test was used for all 2- to 3-months data analysis except mesangial proliferation, for which the Kruskal–Wallis test with Dunn's multiple comparisons was used. For 10- to 12-months data, *t* test was used for mesangial proliferation, Mann–Whitney test was used for glomerular inflammation and interstitial inflammation, one-sample *t* test was used for endocapillary proliferation and glomerular capillary wall thickening (with WT set as zero), and Wilcoxon rank sum test was used for all other analyses.

[a] $P<0.05$ versus WT and $fP^{-/-}$.

[b] $P<0.01$ versus WT and $fP^{-/-}$.

[c] $P<0.001$ versus WT, $fP^{-/-}$, $fH^{m/m}$, and $fH^{m/m}/fP^{-/-}$ (normal).

[d] $P<0.001$ versus WT.

progressive GN, and most died between 8 and 12 weeks. Kidneys from all moribund $fH^{m/m}/fP^{-/-}$ mice examined showed diffuse crescentic GN (50%–90% of glomeruli affected) with compressed glomerular tufts, tubular protein casts, extensive interstitial fibrosis, and glomerular and interstitial infiltration of neutrophils and macrophages (Figure 5, E and F and Table 1). Necropsy analysis showed no abnormality in other major organs, except loss of fat cells in peripancreatic fat pad and changes secondary to renal failure, such as cardiac calcification and edema (data not shown). Trace IgG but strong C3 and C9 staining of the glomeruli (Figure 2) argued against the possibility that $fH^{m/m}/fP^{-/-}$ mice died from immune complex-mediated kidney injury. The absence of vasculitis (data not shown) also eliminated a diagnosis of ANCA-mediated GN. Thus, $fH^{m/m}/fP^{-/-}$ mice died from exacerbated and rapidly progressive C3 GN.

$fH^{m/m}/fP^{-/-}$ Mice Have Glomerular Dense Deposits Resembling Human DDD

We next used electron microscopy to examine the pathologic changes in $fH^{m/m}/fP^{-/-}$ mouse kidneys preceding the development of fatal GN. Regardless of the age, WT and $fP^{-/-}$ mouse glomeruli had largely uniform GBM of normal thickness with well defined podocyte foot processes (Figure 6A and Supplemental Figure 3). Segmental effacement of podocyte foot processes, mesangial expansion, and focal subendothelial dense deposits were detected in the kidneys of 8-week-old $fH^{m/m}$ mice (Figure 6B). Nevertheless, $fH^{m/m}$ mouse kidneys appeared relatively healthy at this age. In 12-month-old $fH^{m/m}$ mice, we observed mesangial proliferation and capillary wall interposition, linear and segmental subendothelial electron-dense deposits along the GBM, inflammatory cell infiltration, and substantial effacement of podocyte foot process (Figure 6C and Supplemental Figure 4, A–C). Of interest, we also observed electron-dense particles accumulating in the vascular space adjacent to the subendothelial dense deposits (Supplemental Figure 4C). The identity of these particles is unknown, but they may have contributed to the formation of the subendothelial dense deposits.

In contrast to age-matched $fH^{m/m}$ mice, kidneys of 8-week-old $fH^{m/m}/fP^{-/-}$ mice showed extensive glomerular injury on electron microscopy. The capillary loops were significantly occluded by mesangial expansion and inflammatory cell infiltrates (Figure 6, D–F). The GBM was irregularly thickened and showed diffuse intramembranous and subepithelial dense deposits as well as focal dissolution (Figure 6, D and E and Supplemental Figure 4, D–F). Extensive podocyte foot process effacement was observed in addition to prominent mesangial matrix expansion with dense deposits (Figure 6, D–F and Supplemental Figure 4, D–F). Mesangiolysis and cellular crescents were also present in some sections (Figure 6F). These results confirmed that fP deficiency markedly exacerbated glomerular injury in $fH^{m/m}$ mice. They also showed that fP deficiency altered the pattern of glomerular dense deposits in $fH^{m/m}$ mice from subendothelial to subepithelial and intramembranous (Supplemental Figure 4), which is characteristic of human DDD. Further supporting the

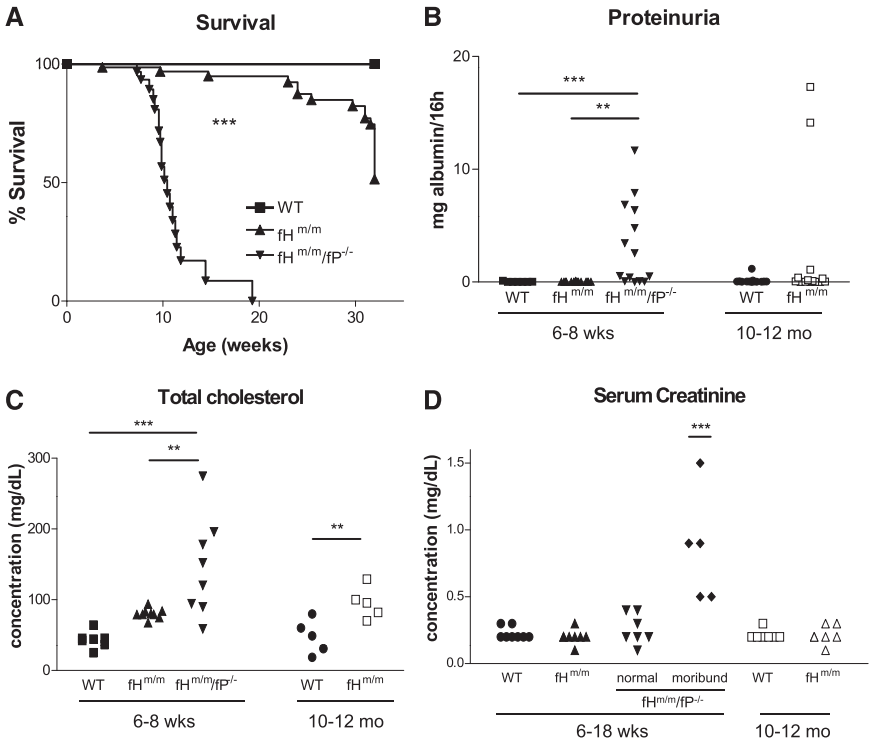

Figure 4. Survival data and kidney function analysis of WT, $fH^{m/m}$, and $fH^{m/m}/fP^{-/-}$ mice. (A) Aggregated survival curves for WT (n=42), $fH^{m/m}$ (n=67), and $fH^{m/m}/fP^{-/-}$ (n=32) mice from multiple cohorts. Although $fH^{m/m}$ showed some mortality by 32 weeks, most $fH^{m/m}/fP^{-/-}$ mice did not survive beyond 14 weeks. ***$P<0.001$; $fH^{m/m}/fP^{-/-}$ versus $fH^{m/m}$, log rank test. (B) Proteinuria was assessed by measuring total albumin in 16-hour urine samples from a cohort of 6- to 8-week-old WT (n=9), $fH^{m/m}$ (n=17), and $fH^{m/m}/fP^{-/-}$ (n=14) mice and a cohort of 10- to 12-month-old WT (n=13) and $fH^{m/m}$ (n=14) mice. **$P\leq0.01$, ***$P<0.001$; Kruskal–Wallis with Dunn's multiple comparison test. (C) Total serum cholesterol was measured in a cohort of 6- to 8-week-old WT (n=7), $fH^{m/m}$ (n=9), and $fH^{m/m}/fP^{-/-}$ (n=8) mice and a cohort of 10- to 12-month-old WT and $fH^{m/m}$ (n=5 for both groups) mice. **$P\leq0.01$, ***$P<0.001$; ANOVA and t test. (D) Serum creatinine was measured in a cohort of 6- to 18-week-old WT (n=8), $fH^{m/m}$ (n=8), and $fH^{m/m}/fP^{-/-}$ (n=12: 7 grossly normal and 5 moribund mice) mice, and a cohort of 10- to 12-month-old WT and $fH^{m/m}$ (n=7 for both groups) mice. ***$P<0.001$ compared with all other groups; ANOVA and t test.

transformation to a DDD-like phenotype, we observed focal dense deposits both within and underneath the Bowman's capsules and tubular basement membranes of $fH^{m/m}/fP^{-/-}$ mice (Supplemental Figure 5).

Antibody Blocking of Properdin in $fH^{m/m}$ Mice Exacerbates C3 GN and Causes Early Death

To confirm the genetic data showing a role of fP in determining the disease phenotype of $fH^{m/m}$ mice, we blocked fP function in $fH^{m/m}$ mice by a neutralizing murine mAb. Starting at 6 weeks, mice were treated for 18 weeks with an anti-fP mAb or an irrelevant isotype control mAb. Figure 7 shows that treatment with the anti-fP mAb, but not the control mAb, caused time-dependent development of proteinuria, hematuria, leukocyturia, and early death. Kidney histology of moribund mice receiving anti-fP mAb showed C3 deposition and diffuse crescentic GN similar to the findings observed in terminal $fH^{m/m}/fP^{-/-}$ mice (Figure 7, E–G). Likewise, ultrastructural changes observed in $fH^{m/m}/fP^{-/-}$ mouse glomeruli, including extensive foot process effacement, irregular GBM thickening, and subepithelial/intramembranous dense deposits, were observed in the kidneys of anti-fP mAb-treated $fH^{m/m}$ mice (Figure 7H and Supplemental Figure 6). Similar histologic and ultrastructural changes were not observed in the glomeruli of control IgG-treated $fH^{m/m}$ mice (Supplemental Figure 7). Thus, pharmacological blockade of fP function in $fH^{m/m}$ mice recapitulated the lethal C3 GN phenotype of $fH^{m/m}/fP^{-/-}$ mice.

Properdin Deficiency Differentially Affects Cell Surface and Fluid-Phase AP Complement Activation and Increases Plasma C3 Levels in $fH^{m/m}$ Mice

To understand the mechanism by which fP deficiency exacerbated C3 GN in $fH^{m/m}$ mice, we compared AP complement activation in $fH^{m/m}$ and $fH^{m/m}/fP^{-/-}$ mice. We found that fP deficiency did not prevent fluid-phase AP complement activation, because $fH^{m/m}/fP^{-/-}$ mice still had very low levels of plasma-intact C3 and fB and elevated levels of activated C3 (Figure 8). Interestingly, however, both ELISA and Western blot assays revealed a significant increase of intact C3 in the plasma of $fH^{m/m}/fP^{-/-}$ mice compared with $fH^{m/m}$ mice (Figure 8, A and B), suggesting that fP deficiency partially decreased AP complement consumption. Furthermore, we observed a markedly different C3 deposition pattern in the $fH^{m/m}/fP^{-/-}$ mouse kidneys (Figure 2). Although C3 deposition in $fH^{m/m}$ mouse glomeruli was both mesangial and along the capillary loops and it was composed of a mixture of granular and linear deposits, C3 staining was brightly linear and restricted to the capillary loops in $fH^{m/m}/fP^{-/-}$ glomeruli (Figure 2). Notably, we found $fH^{m/m}$ mice to have lower plasma fP levels than WT mice (Figure 8C), consistent with fP being consumed in these mice. Immunofluorescence detected prominent glomerular fP staining in $fH^{m/m}$ mice that appeared to be mesangial and partially overlapping with C3 deposition (Supplemental Figure 8). Different C3 deposition patterns were also observed in the livers of these mice. C3 staining in the $fH^{m/m}$ mouse liver had a broader distribution pattern, being present on blood vessel walls as well as cells outside the vascular space (Figure 2). In the $fH^{m/m}/fP^{-/-}$ mouse liver, it was exclusively localized along the vascular

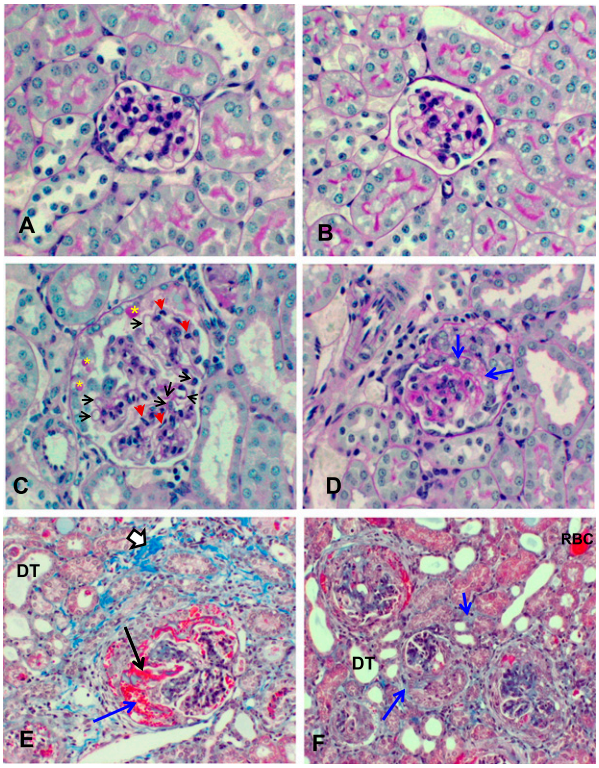

Figure 5. Kidney histology of $fH^{m/m}/fP^{-/-}$ mice. Representative images of PAS staining of glomeruli from (A) WT, (B) $fP^{-/-}$, and (C) $fH^{m/m}/fP^{-/-}$ mice at 2 months (×400). WT and $fP^{-/-}$ glomeruli were healthy, with normal thickness of the GBMs and patent capillary loops, whereas $fH^{m/m}/fP^{-/-}$ glomeruli showed lobulation, thickening of capillary walls (black arrows), and mesangial proliferation and leukocyte infiltration (red arrows). Some $fH^{m/m}/fP^{-/-}$ glomeruli also had parietal cell proliferation with protein globules (yellow asterisks). (D) PAS staining (×400) showing early crescent formation in an 8-week-old $fH^{m/m}/fP^{-/-}$ mouse. (E) Trichrome staining of kidney from a moribund 10-week-old $fH^{m/m}/fP^{-/-}$ mouse (×200) showing extensive crescentic GN. Note the hemorrhage (blue arrow) and fibrinoid necrosis (black arrow) in epithelial crescent. Chronicity is evident by interstitial fibrosis (open arrow) and dilated tubules (DT). (F) Trichrome staining of kidney from a moribund $fH^{m/m}/fP^{-/-}$ mouse (×200) showing the extent of crescent formation. Large epithelial cell crescents are noted in four of five glomeruli in the field. Evidence of hemorrhage and fibrinoid necrosis are again apparent in some crescents. A red blood cell (RBC) cast is observed in one tubule. DT and focal peritubular fibrosis (blue arrows) indicate chronicity of injury.

walls (Figure 2). Collectively, these data suggested that fP deficiency in $fH^{m/m}$ mice abrogated cell surface but not fluid-phase AP complement activation.

To directly test the role of fP in AP complement activation on the cell surface and in the fluid phase, we performed *in vitro* assays, where the function of fH on the cell surface or in the fluid phase was blocked. Figure 9 shows that, in the presence of fH19–20, a recombinant protein that corresponds to the two C-terminal SCR domains of human fH that was previously shown to block fH function on the cell surface,[38] human red blood cells were lysed by autologous serum. This lysis was completely blocked by a neutralizing goat anti-human fP antibody, even in the presence of a neutralizing anti-decay-accelerating factor (DAF) antibody to increase cell sensitivity (Figure 9A). Likewise, in the presence of a murine form of fH19–20 and a neutralizing rabbit anti-mouse Crry antibody, erythrocytes from $DAF^{-/-}CD59^{-/-}$ mice were lysed by normal mouse serum, but lysis was largely prevented in $fP^{-/-}$ serum (Figure 9B). In a separate experiment, we also showed that fP was required for AP complement activation and C3 deposition on the surface of mouse platelets lacking DAF and Crry (Figure 9C). To assess the role of fP in fluid-phase AP complement activation in the absence of fH, we depleted fH from WT and $fP^{-/-}$ mouse sera by affinity chromatography. As shown in Figure 9D, depletion of fH caused similar degrees of C3 activation and consumption in WT and $fP^{-/-}$ mouse sera, confirming that fP was not required for fluid-phase AP complement activation in the absence of fH control.

DISCUSSION

In this study, we have made several important findings that are relevant to the pathogenesis and treatment of fH-related kidney diseases. We showed here that disease phenotype and penetrance of an fH mutation can be significantly enhanced by other changes in the complement cascade. Blocking properdin by either a genetic or pharmacological approach converted the mild C3 GN phenotype of an fH C terminus mutant mouse to lethal and rapidly progressive GN with features of human DDD. Exacerbation of disease in $fH^{m/m}/fP^{-/-}$ mice was rather unexpected and counterintuitive, because recent studies have shown that properdin contributed to tissue injury in several AP complement-mediated disease models; its inhibition in those settings reduced disease severity.[14,32–34]

We have considered several potential explanations for this surprising result. We initially entertained the hypothesis that fP might have an uncharacterized anti-inflammatory function *in vivo* independent of its activity as a facilitator/initiator of AP complement activation. However, the finding that fP deficiency did not affect mortality in $fH^{-/-}$ mice[39] argued against this hypothesis. Thus, the disease-modifying effect of fP deficiency is most striking in $fH^{m/m}$ mice, implying that, although it was ostensibly similar to $fH^{-/-}$ mice in displaying uncontrolled complement activation and age-dependent C3 GN, the $fH^{m/m}$ mice were, in fact, not identical to $fH^{-/-}$ mice. We attribute their phenotypic difference to the small amount of truncated fH present in $fH^{m/m}$ mice (Figure 1E). Indeed, $fH^{m/m}$ mice were found to have significantly higher plasma-intact C3 than $fH^{-/-}$ mice, and the two strains of mice had different patterns of glomerular C3 deposition.[39] Presumably, the residual amount of truncated fH exerted some fluid-phase control to preserve and allow a limited degree of AP complement activation to occur locally in the kidney, where cell surface

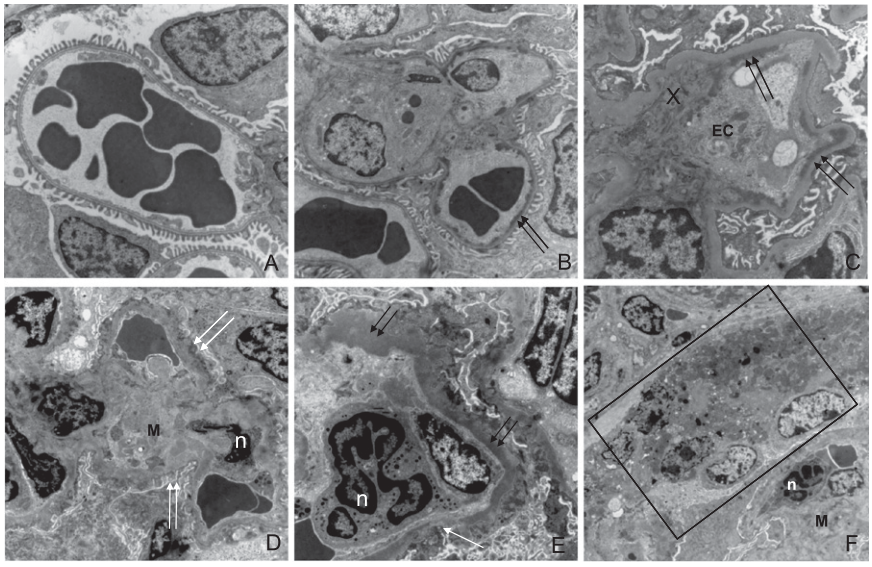

Figure 6. Electron microscopy of WT, $fH^{m/m}$, and $fH^{m/m}/fP^{-/-}$ mouse kidneys showing exacerbated glomerular injury in $fH^{m/m}/fP^{-/-}$ mice. (A) WT mouse glomeruli had normal basement membranes and podocyte foot processes. (B) Glomeruli of young (8 weeks) $fH^{m/m}$ mice had focal subendothelial dense deposits (double black arrows) and mild mesangial expansion but otherwise appeared healthy. (C) By 12 months of age, $fH^{m/m}$ mouse glomeruli showed typical signs of C3 GN, including endothelial injury, significant mesangial proliferation and interposition in addition to foot process effacement and increased subendothelial dense deposits. EC, swollen endothelial cell; X, mesangial interposition. (D–F) The glomeruli of 8-week-old $fH^{m/m}/fP^{-/-}$ mice had marked mesangial expansion, leukocyte infiltration (neutrophils), extensive foot process effacement (white double arrows), irregular GBM thickening with intramembranous dense deposits (black double arrows), and focal GBM dissolution (single white arrow). Epithelial crescents were also observed in some $fH^{m/m}/fP^{-/-}$ glomeruli (boxed area in F). Original magnification, ×10,000 in A, B, and E; ×12,000 in C; ×7500 in D; ×4000 in F. M, mesangial matrix expansion; n, neutrophil.

protection by fH was absent. In contrast, the complete absence of fH in $fH^{-/-}$ mice led to unbridled plasma complement activation and consumption, leaving little C3 to be activated locally in the kidney. This difference may explain why the glomerular C3 staining pattern in $fH^{-/-}$ mice was capillary (deposits of plasma-activated C3), whereas it appeared to be both mesangial and capillary in $fH^{m/m}$ mice (local C3 activation plus deposits of plasma-activated C3) (Figure 2).[39] Thus, although both strains of mice developed age-dependent C3 GN, complement injury in the $fH^{-/-}$ mouse kidney may be instigated mainly by fluid phase-activated complement, whereas both local and fluid-phase complement activation may have contributed to glomerular injury in $fH^{m/m}$ mice.

The key question then is why fP deficiency caused lethal C3 GN in $fH^{m/m}$ but not $fH^{-/-}$ mice. We suspect that this difference is related to different plasma complement levels. $fH^{m/m}$ mice were found to have higher plasma intact C3 than $fH^{-/-}$ mice,[39] presumably because of the presence of residual truncated fH, and fP deficiency further elevated plasma C3 in $fH^{m/m}$ mice (Figure 8). Our interpretation is that lack of fP prevented AP complement activation on many cells of $fH^{m/m}$ mice, which would have reduced C3 consumption, accounting for the significant rise in plasma C3 in these mice (Figure 8). Consistent with this hypothesis, we observed conspicuous changes in C3 staining patterns in the kidney and liver of $fH^{m/m}/fP^{-/-}$ mice compared with $fH^{m/m}$ mice (Figure 2). This hypothesis was further supported by our *in vitro* experiments showing the requirement of fP in AP complement activation on erythrocytes and platelets in the absence of fH and/or membrane regulator protection (Figure 9). Presumably, fP deficiency did not significantly alter plasma C3 level in $fH^{-/-}$ mice, because as discussed above, AP complement was overwhelmingly consumed in the fluid phase; accordingly, there was little C3 activation on the cell surface in $fH^{-/-}$ mice in the first place.[39]

The elevated plasma C3 in $fH^{m/m}/fP^{-/-}$ mice points to mechanisms of lethal C3 GN. Our *in vitro* data showed fP to be dispensable for fluid-phase complement activation caused by fH deficiency (Figure 9). Thus, abrogation of cell surface C3 activation in $fH^{m/m}/fP^{-/-}$ mice could have made more C3 available to be activated in the plasma. However, based on the survival data of $fH^{-/-}$ and $fH^{-/-}/fP^{-/-}$ mice,[39] increased plasma complement activation *per se* in $fH^{m/m}/fP^{-/-}$ mice was unlikely to be the explanation for their lethal GN phenotype. Our data support several readily testable hypotheses. First, with elevated plasma C3 activation, the small amount of truncated fH in $fH^{m/m}/fP^{-/-}$ mice might have helped to generate more iC3b than in $fH^{m/m}$ or $fH^{-/-}/fP^{-/-}$ mice. Previous studies of an $fH^{-/-}/fI^{-/-}$ mouse have indicated the critical role of iC3b in the pathogenesis of C3 GN in $fH^{-/-}$ mice.[40,41] Second, although we showed that fP was required for complement activation on susceptible erythrocytes, platelets, kidney mesangium, and liver cells, it is possible that fP was not essential on certain host cell surfaces, such as podocytes and the GBM. Mouse fP is known to be critical for AP complement activation on some foreign surfaces (*e.g.*, LPS) but not others (*e.g.*, zymosan).[14] Thus, increased plasma C3 in $fH^{m/m}/fP^{-/-}$ mice could have produced more fP-independent activation on podocytes and GBM in the absence of fH protection, leading to lethal C3 GN. Presumably, a DDD-like C3 GN phenotype, rather than aHUS (as seen in $fH^{-/-}$.fHΔ16–20 mice),[42] was observed in $fH^{m/m}/fP^{-/-}$ mice, because endothelial cells and platelets, the main target cells injured in aHUS, were spared because of fP deficiency (Figure 9). Finally, it is possible that a combination of increased plasma and glomerular complement activation was responsible for the lethal C3 GN in $fH^{m/m}/fP^{-/-}$ mice. This finding could explain why $fH^{-/-}$.fHΔ16–20 mice

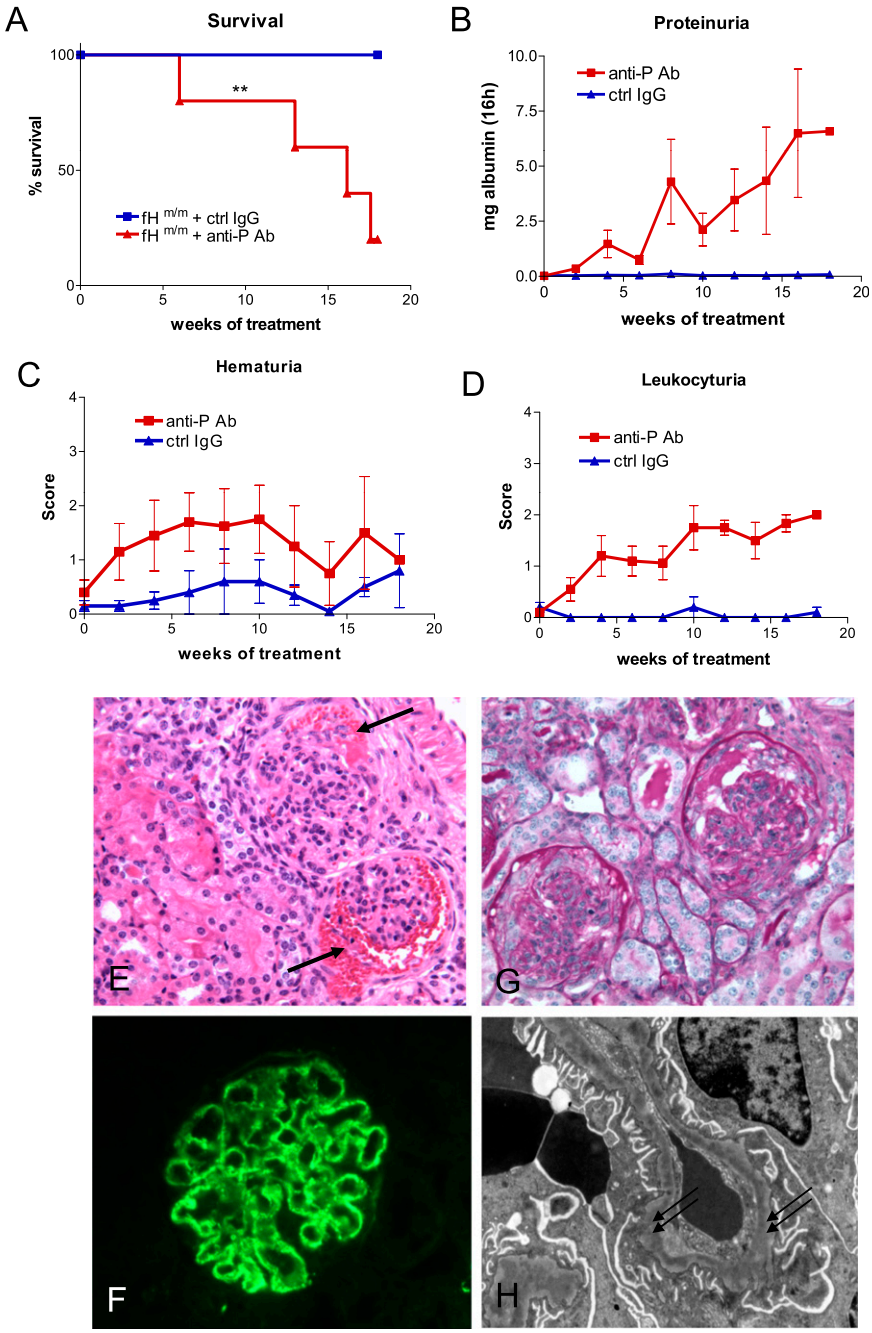

Figure 7. Antibody blocking of fP in $fH^{m/m}$ mice exacerbates C3 GN and causes early death. (A) Survival curves of $fH^{m/m}$ mice treated with anti-P Ab (red) and a control mAb (ctrl IgG; blue; n=5 for each treatment). **P=0.01; log rank test. (B–D) Measurement of renal function over the course of antibody treatment showing impaired renal function in mice receiving anti-P but not the control mAb, which is indicated by the development of (B) proteinuria, (C) hematuria, and (D) leukocyturia. (E–H) Representative light and immunofluorescence microscopy of renal pathology in moribund anti-P mAb-treated mice. (E) Hematoxylin/eosin staining showed glomerular crescents with hemorrhage (black arrows), proliferative changes, and interstitial injury. (F) PAS staining revealed membrane thickening and tubular protein casts. (G) Immunofluorescence staining showed C3 deposition in capillary loops as seen in $fH^{m/m}/fP^{-/-}$ mice. (H) Electron microscopy showed severe podocyte injury and irregular GBM thickening with intramembranous dense deposits (double black arrows). Original magnification, ×400 for E–G; ×12,000 for H.

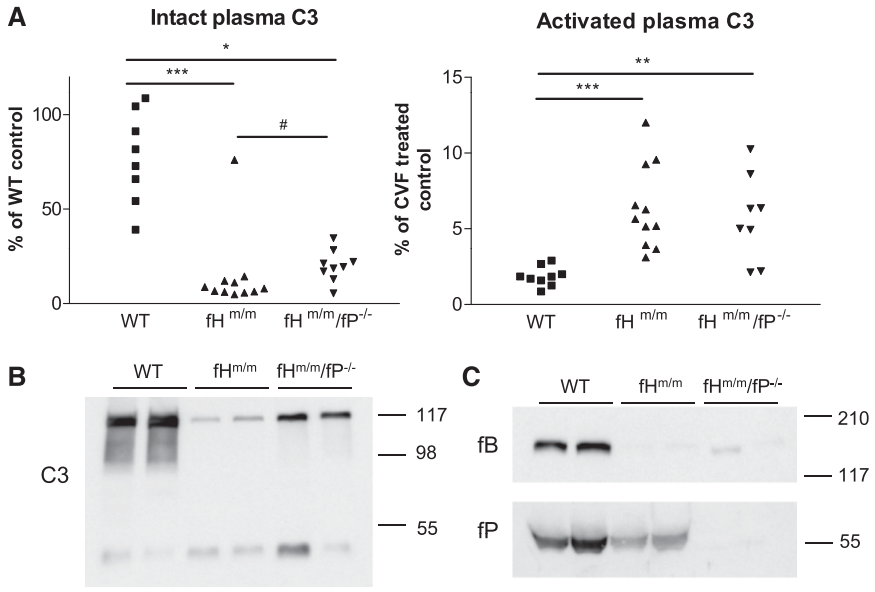

Figure 8. Properdin deficiency did not prevent plasma AP complement activation in $fH^{m/m}$ mice. (A) Both 2-month-old $fH^{m/m}$ (n=11) and $fH^{m/m}/fP^{-/-}$ (n=9) mice had very low plasma-intact C3 levels but elevated plasma-activated C3 levels compared with WT littermates (n=8). *P<0.05, **P<0.01, ***P<0.001. Data analyzed for intact C3 by Kruskal–Wallis test, and data analyzed for activated C3 by ANOVA. Intact C3 levels in $fH^{m/m}/fP^{-/-}$ mice were also significantly higher than the levels in $fH^{m/m}$ mice. #P=0.02; Mann–Whitney test. Values were normalized to reference samples as described in Figure 1. (B and C) Western blotting analysis of (B) plasma C3 and (C) fB and properdin in 2-month-old WT, $fH^{m/m}$, and $fH^{m/m}/fP^{-/-}$ mice, confirming a higher amount of intact C3 α-chain in $fH^{m/m}/fP^{-/-}$ than $fH^{m/m}$ mice. It also shows a lower level of plasma fP in $fH^{m/m}$ than WT mice.

developed aHUS instead of lethal C3 GN, because plasma complement activation was largely prevented in these mice.[42]

Although to our knowledge, no combined fH C-terminal mutation and fP deficiency has yet been identified in human C3 glomerulopathy patients, our animal model data shed significant new light on the pathogenesis of fH mutation-related kidney pathologies and have direct therapeutic implications for human patients. Several recent studies have shown a key role of fP in AP complement-mediated tissue injury, providing a strong rationale for anti-fP therapy in these conditions.[14,32–34,43] Our data presented here suggest that anti-fP therapy may be contraindicated in some fH-related C3 glomerulopathies and highlight the importance of target validation in the development of complement-modulating drugs. The fact that C3 GN caused by an fH mutation can be exacerbated by other factors in complement control may not be unique to fP deficiency. Both the published $fH^{-/-}$.fHΔ16–20 model[42] and the $fH^{m/m}/fP^{-/-}$ model described here suggest that any genetic variations or therapeutic manipulations affecting the balance of plasma and cell surface complement activation could potentially aggravate or change the disease course of an fH-related pathology. This conclusion may help explain the well recognized disease heterogeneity of fH mutations in human patients and suggests a need for careful patient selection based on underlying etiology in conducting clinical trials of anticomplement therapy for C3 glomerulopathy.

CONCISE METHODS

Mice

The generation of $fH^{m/m}$ mice by gene targeting is described in Supplemental Text. WT C57BL/6, enhanced flippase (FLPe) transgenic and $C4^{-/-}$ mice were purchased from the Jackson Laboratory. The generation and source of $fB^{-/-}$, $fP^{-/-}$, $DAF^{-/-}/Crry^{-/-}/C3^{-/-}$, and $DAF^{-/-}/CD59^{-/-}$ mice were reported previously.[14,31,44–46] $C4^{-/-}$, $fB^{-/-}$, and $DAF^{-/-}/CD59^{-/-}$ mice were on a C57BL/6 background, whereas $DAF^{-/-}/Crry^{-/-}/C3^{-/-}$, $fP^{-/-}$, $fH^{m/m}$, and $fH^{m/m}/fP^{-/-}$ mice were on a C57BL/6–129J mixed background. All experiments used age-matched littermates as controls.

C3 ELISA Assays

To measure activated C3 fragments, 96-well ELISA plates were coated with 2.5 μg/ml anti-mouse C3 mAb 3/26 (Hycult Biotechnology) in 0.1 M carbonate buffer overnight at 4°C. The mAb 3/26 recognizes C3b/iC3b/C3c but not intact mouse C3.[47] Plates were washed after each step with PBS/0.5% Tween-20 (PBS-T). Plates were then blocked with 1% BSA-PBS for 1 hour at room temperature (RT) followed by the addition of serially diluted mouse plasma samples in 1% BSA-PBS starting at 1:50. Positive control was a cobra venom factor (CVF)-treated serum, with serial dilutions starting at 1:500. After incubation with plasma for 1 hour at RT, the plate was washed three times with PBS-T and then incubated with horseradish peroxidase goat anti-mouse C3 Ab (1:4000; MP Biomedicals) for 1 hour at RT. After washing, the plate was developed using OptEIA substrate (BD Biosciences). All samples were normalized to CVF-treated serum control.

For intact C3, plates were coated with 2.5 μg/ml anti-mouse C3 mAb 11H9 (Hycult Biotechnology) in 0.1 M carbonate buffer overnight at 4°C. The mAb 11H9 recognizes intact C3 as well as C3b/iC3b.[48] Plates were then blocked with 1% BSA-PBS for 1 hour at RT followed by the addition of serially diluted mouse plasma samples starting at 1:50 in 1% BSA-PBS. Positive control was WT plasma (same plasma used for all plates). After incubation with plasma for 1 hour at RT, plates were washed three times with PBS-T and then incubated with a rabbit polyclonal anti-mouse C3a Ab (provided by John Lambris, University of Pennsylvania; 1:1000) for 1 hour at RT. Finally, plates were incubated with horseradish peroxidase goat anti-rabbit IgG Ab (1:4000; Bio-Rad) for 1 hour at RT. After washing, plates were developed using OptEIA substrate (BD Biosciences). All samples were normalized to a WT plasma control.

Survival Curve

Survival was assessed in WT, $fH^{m/m}$, and $fH^{m/m}/fP^{-/-}$ until 8 months of age. Data were categorized as being censored (euthanized) or natural death and analyzed by GraphPad Prism (La Jolla,

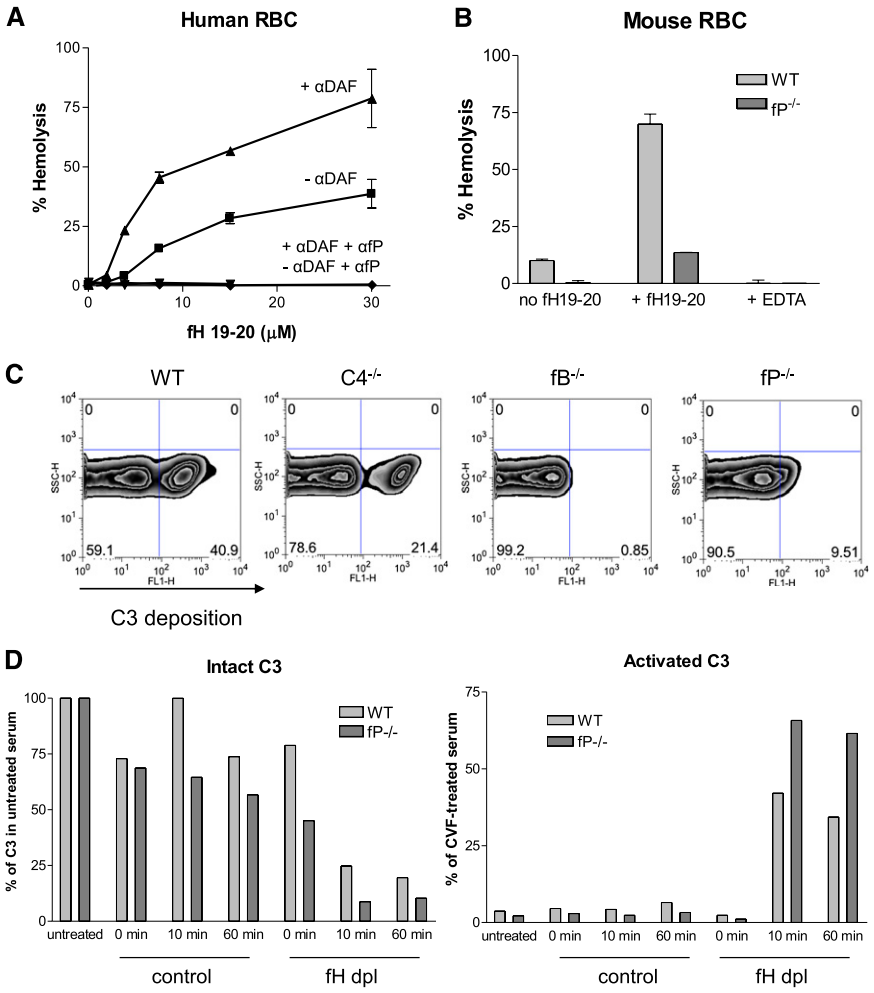

Figure 9. Properdin is critical for AP complement activation on autologous cells but not in the fluid phase. (A) Human red blood cells were lysed in 50% normal human serum in the presence of fH SCR19–20. Addition of an anti-DAF (αDAF) antibody increased lysis. In both cases, lysis was prevented by an anti-properdin (αfP) antibody. ■, fH SCR19–20; ▲, fH SCR19–20 + anti-DAF; ◆, fH SCR19–20 + anti-fP; ▼, fH SCR19–20 + anti-DAF + anti-fP. Assays were performed in triplicates. (B) $DAF^{-/-}CD59^{-/-}$ mouse erythrocytes were lysed by 50% WT mouse serum in the presence of mouse fH SCR19–20 and an anti-Crry antibody (+ fH19–20). Lysis was largely prevented if $fP^{-/-}$ mouse serum was used in the same assay (+ fH19–20). No lysis occurred if EDTA was included in the assays (+ EDTA) or if fH SCR19–20 was omitted (no fH19–20). Assays were performed in duplicates. Data in A and B are normalized to the optical density of osmotically lysed erythrocytes. (C) FACS analysis of C3 deposition on $DAF^{-/-}/Crry^{-/-}/C3^{-/-}$ mouse platelets incubated with serum *in vitro*. Significant C3 deposition occurred on platelets incubated with WT and $C4^{-/-}$ mouse sera but not $fB^{-/-}$ or $fP^{-/-}$ mouse sera, suggesting properdin-dependent AP complement activation on the platelets. Numbers indicate the percentage of cells in each quadrant. Data in A–C are representative of at least three independent experiments. (D) C3 activation in fH-depleted mouse serum is properdin-independent. Both WT (light gray bars) and $fP^{-/-}$ (dark gray bars) mouse serum incurred time-dependent C3 activation after passing through an anti-fH mAb column to deplete fH (fH dpl) but not after passing through a control mAb column (control). Values for activated C3 were normalized to a reference sample as described in Figure 1, and intact C3 was normalized to C3 in the original serum before affinity column processing. Data are representative of three independent experiments.

CA) using the Mantel–Haenszel log rank test as described previously.[49]

Measurement of Renal Function

Serum creatinine was analyzed by a Vitros 350 chemistry analyzer (Johnson & Johnson). Total serum cholesterol was determined by the Cholesterol E kit according to the manufacturer's protocol (Wako Chemicals). Plasma and urine albumin were quantified using a mouse albumin ELISA kit according to the manufacturer's instructions (Bethyl Laboratories). Urine samples were collected in metabolic cages for 16 hours, and volumes were recorded. Total urine albumin was determined by multiplying albumin concentration (determined by ELISA) by total urine volume per 16 hours.

Grading of Renal Pathology

The renal sections, each stained with hematoxylin/eosin and PAS and some stained with trichrome, were interpreted as an unknown sample. The following glomerular changes were recorded: mesangial thickening and cell proliferation, glomerular inflammation indicated by granulocytes and intracapillary mononuclear cells, endocapillary proliferation in glomerulus, glomerular capillary wall thickening, epithelial crescent formation, and glomerular sclerosis. In addition, interstitial inflammation and arteriosclerosis were determined. The severity of each change was graded from zero to four, with four being most severe and zero being normal. The percentage of glomeruli among 50 that showed epithelial crescents was scored, and the fraction of the cortical area that showed interstitial fibrosis and tubular atrophy was scored.

Properdin Inhibition in $fH^{m/m}$ Mice

Beginning at 6 weeks of age, $fH^{m/m}$ mice were treated weekly (1 mg/mouse intraperitoneally) with mAb 14E1, a function-blocking mouse anti-mouse fP IgG (anti-P Ab).[50] The dosage and frequency of mAb treatment was determined in pilot studies to be sufficient for *in vivo* inhibition of fP activity as described.[50] A control group of $fH^{m/m}$ mice was given an irrelevant isotype control mouse IgG1 antibody (purified from MoPC 31C hybridoma; ATCC) on the same dosing schedule as the anti-P Ab-treated mice. Mice were treated for a total of 18 weeks, and survival was assessed over the course of the experiment as described above. To assess renal function, plasma and urine samples were collected every 2 weeks. Urine albumin was measured as described above. Additionally, hematuria

and leukocyturia were assessed semiquantitatively using color indicator strips (Uristix; Siemens).

fH Depletion from Mouse Serum

fH was depleted from WT and $fP^{-/-}$ mouse sera by affinity chromatography. To prepare affinity columns, 2 mg monoclonal mouse anti-mouse fH antibody (clone 18–7; generated in house) or an irrelevant isotope control mouse IgG1 mAb was coupled to 150 mg cyanogen bromide (CNBr)-activated sepharose according to standard procedures (GE Healthcare Life Sciences). An affinity column was prepared by packing 200 μl antibody-coupled beads into a spin column and washing three times with PBS. Mouse serum (200 μl 50% serum diluted in gelatin veronal-buffered saline $[GVB]^{++}$ buffer) was added into the column and incubated for 2 minutes at 4°C. Afterward, the column was quickly spun for 2 minutes at 5000 rpm and 1 minute at 4°C, and flow-through was collected. Flow-through was then incubated for different time periods (0, 10, or 60 minutes) at 37°C, and at the end of the incubation, AP complement activation was stopped with the addition of an equal volume of GVB^{++} with 20 mM EDTA. Intact and activated C3 levels in the serum samples were then measured by ELISA as described above.

Statistical Analyses

Data were analyzed with GraphPad software by two-tailed *t* test and one-way ANOVA with Tukey test for parametric data as indicated. For nonparametric data, the Mann–Whitney and Kruskal–Wallis with Dunn's multiple comparison tests were used. Normality of data was assessed by the Kolmogorov–Smirnov test. A *P* value less than 0.05 was considered statistically significant. Error bars indicate SEM unless indicated otherwise.

ACKNOWLEDGMENTS

We thank Drs. Matthew Pickering and Marieta Ruseva (Imperial College of London) for useful discussions and critical review of the manuscript, Dr. John Lambris for anti-C3a antibody, Drs. Piere Russo, Suxia Wang, Mark Haas, and John Tomaszewski for consultation on renal histology and pathology, Jasmine Zhao and the Cell and Developmental Biology microscopy core for help with confocal imaging, Ray Meade and the Electron Microscopy Resource Laboratory for help with electron microscopy analysis, and the Clinical Pathology laboratory at the Veterinary Hospital of the University of Pennsylvania for serum creatinine measurement.

This work is supported by National Institutes of Health Grants AI085596, AI44970, and AI49344, a predoctoral fellowship from the American Heart Association (to A.M.L.), and a grant from the Kidneeds Foundation (to W.-C.S.).

Part of this study has been presented in abstract form at the XXIII International Complement Workshop, New York, New York, August 1–5, 2010 and the 13th European Meeting on Complement and Human Diseases, Leiden, The Netherlands, August 21–24, 2011.

DISCLOSURES

None.

REFERENCES

1. Walport MJ: Complement. First of two parts. *N Engl J Med* 344: 1058–1066, 2001
2. Dunkelberger JR, Song WC: Complement and its role in innate and adaptive immune responses. *Cell Res* 20: 34–50, 2010
3. Holers VM: The spectrum of complement alternative pathway-mediated diseases. *Immunol Rev* 223: 300–316, 2008
4. Thurman JM, Holers VM: The central role of the alternative complement pathway in human disease. *J Immunol* 176: 1305–1310, 2006
5. Kim DD, Song WC: Membrane complement regulatory proteins. *Clin Immunol* 118: 127–136, 2006
6. Song WC: Complement regulatory proteins and autoimmunity. *Autoimmunity* 39: 403–410, 2006
7. Józsi M, Zipfel PF: Factor H family proteins and human diseases. *Trends Immunol* 29: 380–387, 2008
8. Rodríguez de Córdoba S, Esparza-Gordillo J, Goicoechea de Jorge E, Lopez-Trascasa M, Sánchez-Corral P: The human complement factor H: Functional roles, genetic variations and disease associations. *Mol Immunol* 41: 355–367, 2004
9. Atkinson JP, Goodship TH: Complement factor H and the hemolytic uremic syndrome. *J Exp Med* 204: 1245–1248, 2007
10. Józsi M, Oppermann M, Lambris JD, Zipfel PF: The C-terminus of complement factor H is essential for host cell protection. *Mol Immunol* 44: 2697–2706, 2007
11. Ferreira VP, Herbert AP, Hocking HG, Barlow PN, Pangburn MK: Critical role of the C-terminal domains of factor H in regulating complement activation at cell surfaces. *J Immunol* 177: 6308–6316, 2006
12. Fearon DT, Austen KF: Properdin: Binding to C3b and stabilization of the C3b-dependent C3 convertase. *J Exp Med* 142: 856–863, 1975
13. Spitzer D, Mitchell LM, Atkinson JP, Hourcade DE: Properdin can initiate complement activation by binding specific target surfaces and providing a platform for de novo convertase assembly. *J Immunol* 179: 2600–2608, 2007
14. Kimura Y, Miwa T, Zhou L, Song WC: Activator-specific requirement of properdin in the initiation and amplification of the alternative pathway complement. *Blood* 111: 732–740, 2008
15. Kemper C, Mitchell LM, Zhang L, Hourcade DE: The complement protein properdin binds apoptotic T cells and promotes complement activation and phagocytosis. *Proc Natl Acad Sci U S A* 105: 9023–9028, 2008
16. Hourcade DE: The role of properdin in the assembly of the alternative pathway C3 convertases of complement. *J Biol Chem* 281: 2128–2132, 2006
17. Ferreira VP, Cortes C, Pangburn MK: Native polymeric forms of properdin selectively bind to targets and promote activation of the alternative pathway of complement. *Immunobiology* 215: 932–940, 2010
18. Agarwal S, Ferreira VP, Cortes C, Pangburn MK, Rice PA, Ram S: An evaluation of the role of properdin in alternative pathway activation on Neisseria meningitidis and Neisseria gonorrhoeae. *J Immunol* 185: 507–516, 2010
19. Levy M, Halbwachs-Mecarelli L, Gubler MC, Kohout G, Bensenouci A, Niaudet P, Hauptmann G, Lesavre P: H deficiency in two brothers with atypical dense intramembranous deposit disease. *Kidney Int* 30: 949–956, 1986
20. Servais A, Frémeaux-Bacchi V, Lequintrec M, Salomon R, Blouin J, Knebelmann B, Grünfeld JP, Lesavre P, Noël LH, Fakhouri F: Primary glomerulonephritis with isolated C3 deposits: A new entity which shares common genetic risk factors with haemolytic uraemic syndrome. *J Med Genet* 44: 193–199, 2007
21. Smith RJ, Harris CL, Pickering MC: Dense deposit disease. *Mol Immunol* 48: 1604–1610, 2011
22. Fakhouri F, Frémeaux-Bacchi V, Noël LH, Cook HT, Pickering MC: C3 glomerulopathy: A new classification. *Nat Rev Nephrol* 6: 494–499, 2010
23. Caprioli J, Noris M, Brioschi S, Pianetti G, Castelletti F, Bettinaglio P, Mele C, Bresin E, Cassis L, Gamba S, Porrati F, Bucchioni S, Monteferrante G, Fang CJ, Liszewski MK, Kavanagh D, Atkinson JP, Remuzzi G; International

Registry of Recurrent and Familial HUS/TTP: Genetics of HUS: The impact of MCP, CFH, and IF mutations on clinical presentation, response to treatment, and outcome. *Blood* 108: 1267–1279, 2006
24. Pickering M, Cook HT: Complement and glomerular disease: New insights. *Curr Opin Nephrol Hypertens* 20: 271–277, 2011
25. de Córdoba SR, de Jorge EG: Translational mini-review series on complement factor H: Genetics and disease associations of human complement factor H. *Clin Exp Immunol* 151: 1–13, 2008
26. Kavanagh D, Goodship TH, Richards A: Atypical haemolytic uraemic syndrome. *Br Med Bull* 77-78: 5–22, 2006
27. Ferreira VP, Herbert AP, Cortés C, McKee KA, Blaum BS, Esswein ST, Uhrín D, Barlow PN, Pangburn MK, Kavanagh D: The binding of factor H to a complex of physiological polyanions and C3b on cells is impaired in atypical hemolytic uremic syndrome. *J Immunol* 182: 7009–7018, 2009
28. Hilleren P, Parker R: Mechanisms of mRNA surveillance in eukaryotes. *Annu Rev Genet* 33: 229–260, 1999
29. Hilleren P, Parker R: mRNA surveillance in eukaryotes: Kinetic proofreading of proper translation termination as assessed by mRNP domain organization? *RNA* 5: 711–719, 1999
30. Baker KE, Parker R: Nonsense-mediated mRNA decay: Terminating erroneous gene expression. *Curr Opin Cell Biol* 16: 293–299, 2004
31. Pickering MC, Cook HT, Warren J, Bygrave AE, Moss J, Walport MJ, Botto M: Uncontrolled C3 activation causes membranoproliferative glomerulonephritis in mice deficient in complement factor H. *Nat Genet* 31: 424–428, 2002
32. Dimitrova P, Ivanovska N, Schwaeble W, Gyurkovska V, Stover C: The role of properdin in murine zymosan-induced arthritis. *Mol Immunol* 47: 1458–1466, 2010
33. Zhou HF, Yan H, Stover CM, Fernandez TM, Rodriguez de Cordoba S, Song WC, Wu X, Thompson RW, Schwaeble WJ, Atkinson JP, Hourcade DE, Pham CT: Antibody directs properdin-dependent complement alternative pathway activation in a mouse model of abdominal aortic aneurysm. *Proc Natl Acad Sci U S A* 109: E415–E422, 2012
34. Kimura Y, Zhou L, Miwa T, Song WC: Genetic and therapeutic targeting of properdin in mice prevents complement-mediated tissue injury. *J Clin Invest* 120: 3545–3554, 2010
35. Nakatsue T, Koike H, Han GD, Suzuki K, Miyauchi N, Yuan H, Salant DJ, Gejyo F, Shimizu F, Kawachi H: Nephrin and podocin dissociate at the onset of proteinuria in experimental membranous nephropathy. *Kidney Int* 67: 2239–2253, 2005
36. Hamano Y, Grunkemeyer JA, Sudhakar A, Zeisberg M, Cosgrove D, Morello R, Lee B, Sugimoto H, Kalluri R: Determinants of vascular permeability in the kidney glomerulus. *J Biol Chem* 277: 31154–31162, 2002
37. Mundel P, Shankland SJ: Podocyte biology and response to injury. *J Am Soc Nephrol* 13: 3005–3015, 2002
38. Ferreira VP, Pangburn MK: Factor H mediated cell surface protection from complement is critical for the survival of PNH erythrocytes. *Blood* 110: 2190–2192, 2007
39. Ruseva MM, Vernon KA, Lesher AM, Schwaeble WJ, Youssif YA, Botto M, Cook HT, Song WC, Stover C, Pickering MC: Properdin deficiency exacerbates C3 glomerulopathy in factor H-deficient mice. *J Am Soc Nephrol* 24: 43–52, 2013
40. Rose KL, Paixao-Cavalcante D, Fish J, Manderson AP, Malik TH, Bygrave AE, Lin T, Sacks SH, Walport MJ, Cook HT, Botto M, Pickering MC: Factor I is required for the development of membranoproliferative glomerulonephritis in factor H-deficient mice. *J Clin Invest* 118: 608–618, 2008
41. Paixão-Cavalcante D, Hanson S, Botto M, Cook HT, Pickering MC: Factor H facilitates the clearance of GBM bound iC3b by controlling C3 activation in fluid phase. *Mol Immunol* 46: 1942–1950, 2009
42. Pickering MC, de Jorge EG, Martinez-Barricarte R, Recalde S, Garcia-Layana A, Rose KL, Moss J, Walport MJ, Cook HT, de Córdoba SR, Botto M: Spontaneous hemolytic uremic syndrome triggered by complement factor H lacking surface recognition domains. *J Exp Med* 204: 1249–1256, 2007
43. Kemper C, Atkinson JP, Hourcade DE: Properdin: Emerging roles of a pattern-recognition molecule. *Annu Rev Immunol* 28: 131–155, 2010
44. Yamada K, Miwa T, Liu J, Nangaku M, Song W-C: Critical protection from renal ischemia reperfusion injury by CD55 and CD59. *J Immunol* 172: 3869–3875, 2004
45. Molina H, Miwa T, Zhou L, Hilliard B, Mastellos D, Maldonado MA, Lambris JD, Song WC: Complement-mediated clearance of erythrocytes: Mechanism and delineation of the regulatory roles of Crry and DAF. Decay-accelerating factor. *Blood* 100: 4544–4549, 2002
46. Matsumoto M, Fukuda W, Circolo A, Goellner J, Strauss-Schoenberger J, Wang X, Fujita S, Hidvegi T, Chaplin DD, Colten HR: Abrogation of the alternative complement pathway by targeted deletion of murine factor B. *Proc Natl Acad Sci U S A* 94: 8720–8725, 1997
47. Mastellos D, Prechl J, László G, Papp K, Oláh E, Argyropoulos E, Franchini S, Tudoran R, Markiewski M, Lambris JD, Erdei A: Novel monoclonal antibodies against mouse C3 interfering with complement activation: Description of fine specificity and applications to various immunoassays. *Mol Immunol* 40: 1213–1221, 2004
48. Kremmer E, Thierfelder S, Felber E, Hoffmann-Fezer G, Wasiliu M: Monoclonal antibodies to complement components without the need of their prior purification. II. Antibodies to mouse C3 and C4. *Hybridoma* 9: 309–317, 1990
49. Altman DG: *Practical Statistics for Medical Research*, Oxford, United Kingdom, Chapman & Hall, 1991
50. Miwa T, Sato S, Gullipalli D, Nangaku M, Song WC: Blocking properdin and the alternative pathway complement ameliorates renal ischemia reperfusion injury in decay-accelerating factor and CD59 double knockout mice. *J Immunol* 2012, in press

See related editorial, "Unexpected Role for Properdin in Complement C3 Glomerulopathies," on pages 5–7.

This article contains supplemental material online at http://jasn.asnjournals.org/lookup/suppl/doi:10.1681/ASN.2012060570/-/DCSupplemental.